Primary α and secondary β relaxation dynamics of meta-toluidine in the liquid state investigated by broadband dielectric spectroscopy

H. Švajdlenková, A. Ruff, P. Lunkenheimer, A. Loidl, and J. Bartoš

Citation: The Journal of Chemical Physics **147**, 084506 (2017); doi: 10.1063/1.5000257
View online: http://dx.doi.org/10.1063/1.5000257
View Table of Contents: http://aip.scitation.org/toc/jcp/147/8
Published by the American Institute of Physics

Primary α and secondary β relaxation dynamics of *meta-toluidine* in the liquid state investigated by broadband dielectric spectroscopy

H. Švajdlenková,[1] A. Ruff,[2] P. Lunkenheimer,[2] A. Loidl,[2] and J. Bartoš[1]
[1]*Polymer Institute of SAS, Dúbravská cesta 9, SK-845 41 Bratislava, Slovak Republic*
[2]*Experimental Physics V, University of Augsburg, D-861 35 Augsburg, Germany*

(Received 17 May 2017; accepted 14 August 2017; published online 30 August 2017)

We report a broadband dielectric spectroscopic (BDS) study on the clustering fragile glass-former *meta-toluidine (m-TOL)* from 187 K up to 289 K over a wide frequency range of 10^{-3}–10^{9} Hz with focus on the primary α relaxation and the secondary β relaxation *above* the glass temperature T_g. The broadband dielectric spectra were fitted by using the Havriliak-Negami (HN) and Cole-Cole (CC) models. The β process disappearing at $T_{\beta,disap} = 1.12T_g$ exhibits non-Arrhenius dependence fitted by the Vogel-Fulcher-Tamman-Hesse equation with $T_{0\beta}{}^{VFTH}$ in accord with the characteristic differential scanning calorimetry (DSC) limiting temperature of the glassy state. The essential feature of the α process consists in the distinct changes of its spectral shape parameter β_{HN} marked by the characteristic BDS temperatures $T_{B1}{}^{\beta HN}$ and $T_{B2}{}^{\beta HN}$. The primary α relaxation times were fitted over the entire temperature and frequency range by several current three-parameter up to six-parameter dynamic models. This analysis reveals that the crossover temperatures of the idealized mode coupling theory model ($T_c{}^{MCT}$), the extended free volume model ($T_0{}^{EFV}$), and the two-order parameter (TOP) model ($T_m{}^{c}$) are close to $T_{B1}{}^{\beta HN}$, which provides a consistent physical rationalization for the first change of the shape parameter. In addition, the other two characteristic TOP temperatures $T_0{}^{TOP}$ and T_A are coinciding with the thermodynamic Kauzmann temperature T_K and the second change of the shape parameter at around $T_{B2}{}^{\beta HN}$, respectively. These can be related to the onset of the *liquid*-like domains in the glassy state or the disappearance of the *solid*-like domains in the normal liquid state. *Published by AIP Publishing.* [http://dx.doi.org/10.1063/1.5000257]

I. INTRODUCTION

The long-term challenge and the still unresolved problem in condensed and soft matter physics are to understand the *chemical structure* vs. *physical structure* and *dynamic relationships* in various types of disordered systems.[1–3] One of the basic questions concerns the physical mechanism controlling the evolution of the physical structure and dynamics from the equilibrated stable (normal) liquid state to the non-equilibrated glassy state at the glass transition temperature, T_g, through the equilibrated metastable supercooled liquid state.

The universal features of the structural dynamics of various types of glass-forming liquids as obtained from broadband dielectric spectroscopy (BDS)[4,5] are deviations from the "ideal" Debye and Arrhenius laws dealing with the time behavior of the relaxing variable or with the temperature behavior of the relaxation times, respectively. Moreover, some detailed dynamic studies performed on a variety of organic glass formers over a wide temperature range revealed several regions of distinct viscosity and structural relaxation time behavior which are marked by several characteristic dynamic (crossover) temperatures, $T_{A,B}{}^{DYN}$, such as the Arrhenius T_A,[6–8] Stickel $T_B{}^{ST}$,[9] and Schönhals $T_B{}^{SCH}$[10] temperatures. Another aspect in the dielectric response expressed by the coefficient of non-exponentiality, β_{KWW}, of the Kohlrausch-Williams-Watts (KWW) time function or the related shape coefficients in the general Havriliak-Negami (HN) frequency function exhibits also often various regions of the distinct behavior marked by the characteristic temperature $T_B{}^{\beta KWW}$.[11,12] All these dynamic findings indicate a non-monotonic slowing down of the structural relaxation with the existence of dynamic heterogeneity and qualitative changes in molecular motion of organic glass formers.

To explain the structural dynamics of organic glass formers and the afore-mentioned crossover and transition phenomena, several approaches based on the extended free volume (EFV) model,[13,14] the coupling model (CM),[15,16] and mode coupling theory (MCT)[17] were proposed. Some time ago, the presence of cluster-like heterogeneities in a few amorphous glass formers was uncovered by the combination of diffraction and computer modeling,[18] and this finding was plausibly explained in terms of the hetero-phase fluctuation (HPF) model.[19] A similar approach is represented by the two-order parameter (TOP) model[20] based on the idea about the co-existence and mutual interplay of three dynamic structures in a glass-forming material, i.e., local favored structures (LFSs) and *solid*-like and *liquid*-like domains.

Recently, the last model was utilized to describe and interpret the detailed BDS data over extraordinary wide temperature ranges on a series of small molecular glass-formers of different types such as *propylene carbonate*[21] and a series of *propylene glycols*[22] and *salol*[23] as well as

on a few amorphous *homo-* and *heteropolymers* such as *poly(propylene glycol)*,[24] *cis-trans-1,4-poly(butadiene)*,[25] and *poly(vinylmethylether)*.[26] These systematic BDS and TOP studies revealed the relationships between the temperature development of *solid*-like domains and the slowing down of the primary α dynamics[20–26] as well as that and the boundary or crossover temperatures of the secondary relaxation.[22–25] In some cases, the TOP model provides plausible descriptions not only of the structural relaxation time over a wide temperature range of the non-Arrhenius behavior but also of other spectral parameters of the structural relaxation such as shape width and the relaxation strength.[20,22–24]

meta-Toluidine (m-TOL) is a small molecular organic glass former with several interesting thermodynamic,[27,28] structural,[29–31] and dynamic[32–45] properties such as (i) a low crystallization ability, (ii) a strong tendency to create molecular clusters via intermolecular H-bonding, and—at the same time—(iii) the relatively high fragility $m_g = 79$[28] or 84[41] and $F_{1/2} = 0.80$[38] or 0.73.[41]

From the previous DSC studies, it follows that *m-TOL* does not exhibit "hot" crystallization on slow cooling, even at the cooling rate of −10 K/day.[27] On the other hand, the character of the DSC response on heating depends on the preparation mode of the glassy state being strongly influenced by the final cooled temperature in the glassy state. The limited temperature for the occurrence of the so-called "cold" crystallization on heating of *m-TOL* is around 130 K.[28] The glass transition temperature of the amorphous *m-TOL* sample and the melting point of the cold-crystallized *m-TOL* one were determined at a heating rate 10 K/min to be $T_g^{DSC} = 187$ K and $T_m^{DSC} = 243$ K, respectively.[27,28]

One of the important assumptions of the physical picture behind the TOP model is the existence of the so-called local favored structures (LFSs) in the liquid state which can be ascribed to the so-called pre-peak in the structure factor from x-ray or neutron diffraction. A detailed structural study of *m-TOL* indicates the medium-range order of its molecules with the formation of clusters.[29] This finding was supported by extensive Monte Carlo (MC)[30] and molecular dynamic (MD) simulations.[31]

As for the dynamics of *m-TOL*, several techniques were applied such as viscosity,[32,33] light,[34–36] inelastic x-ray,[37] and neutron scattering[38] and mechanical and dielectric relaxation spectroscopy.[39–45] The first dielectric study on *m-TOL* performed by Cutroni *et al.*[40] addressed the primary α process over a wide frequency range of 5 Hz–2 GHz. They found that the relaxation time data can be described separately in the lower temperature range 193–253 K by the non-Arrhenius equation, i.e., the Vogel-Fulcher-Tamman-Hesse (VFTH) equation[46] for the relaxation time as long as 10^{-3} s and in the higher temperature range 273–323 K by the Arrhenius law for the relaxation times as short as $\sim 10^{-10.5}$ s. As for the relaxation response, they also found a continuous increase of the non-exponentiality coefficient β_{KWW} trend to quasi-saturation with increasing temperature. Later, Mandanici *et al.*[41] focused in detail on the lower frequency broadband dielectric spectra and, in contrary to Ref. 40, the validity of the time-temperature superposition (TTS) principle over a range of 190–215 K, where the relaxation time changes from 1 s down to 10^{-6} s, was found. In addition, they observed for the first time, the secondary β relaxation in the *glassy* state from 130 K up to 160 K exhibiting the usual Arrhenius behavior.[41,42,47]

The aim of our present dielectric study on *m-TOL* is to verify and extend the BDS databases about the primary α process as well as about the secondary β process in the *liquid* state by performing detailed low-frequency LF-BDS and especially high-frequency HF-BDS measurements. In contrast to the previous dielectric spectroscopy works, the distinct behavior of the spectral shape parameter of the structural relaxation has been found. In addition, we present for the first time, the relaxation data on the secondary β process *above* T_g. Finally, several three-parameter up to six-parameter dynamic models were tested in order to describe the structural relaxation time with the aim to also explain the observed temperature dependence of its spectral shape parameter.

II. EXPERIMENTAL PART

A. Material

m-Toluidine (m-TOL) (m-methylaniline, 3-amino-1-methyl benzene) $C_6H_4(CH_3)(NH_2)$ with the purity of 99% from Sigma Aldrich, Inc., Germany, was used. The glass to liquid transition temperature T_g was determined to be 187 K by DSC at the heating rate 10 K/min in accord with Ref. 28.

B. BDS method

The dielectric measurements were carried out at Experimental Physics V, University of Augsburg, by the combination of two devices covering a broad frequency range of 10^{-2}–10^9 Hz. The low-frequency range 10^{-2}–10^7 Hz was monitored with a high resolution Novocontrol dielectric α analyzer. For the frequency range 10^6–10^9 Hz, a coaxial line method and the HP 4291 impedance analyzer have been used.[48,49] For both measurements, the sample of *m-TOL* as received was filled into parallel-plate capacitors. Frequency scans of the complex dielectric function were performed over the temperature range from 187 K to 289 K with steps of 3 or 5 K by using a N_2-gas cryostat.

The dielectric loss spectra were analyzed using the empirical Havriliak-Negami (HN) equation[4,5,50]

$$\varepsilon(\omega) = \sum_i \frac{\Delta\varepsilon_i}{\left[1 + (i\omega\tau_{HN,i})^{1-\alpha_{HN,i}}\right]^{\beta_{HN,i}}} + \varepsilon_\infty, \qquad (1)$$

where $\Delta\varepsilon_i = (\varepsilon_s - \varepsilon_\infty)$ is the relaxation strength of the i-th mode, $\tau_{HN,i}$ is the relaxation time, and $\alpha_{HN,i}$ and $\beta_{HN,i}$ are the shape parameters of the i-th relaxation mode.

As the dielectric spectra of *m-TOL* in the supercooled liquid state exhibit a bimodal form over a certain temperature range, we applied the sum of the HN and Cole-Cole (CC) model functions. The HN function for asymmetric broadening of the spectral peak with the shape parameters $\alpha_{HN} \neq 0$ and $\beta_{HN} \neq 0$ is used for the α relaxation.[4,5,50] The relaxation time related to the position of the maximal loss τ_{max} is calculated by the following formula:[51]

$$\tau_{\max} = \tau_{HN}\left[\frac{\sin\frac{\pi(1-\alpha_{HN})\beta_{HN}}{2(\beta_{HN}+1)}}{\sin\frac{\pi(1-\alpha_{HN})}{2(\beta_{HN}+1)}}\right]^{1/(1-\alpha_{HN})}. \quad (2)$$

In the case of symmetric broadening of the spectral peak, Eq. (1) with the shape parameters $\beta_{HN} = \beta_{CC} = 1$ and $\alpha_{HN} = \alpha_{CC} \neq 0$ transforms into the Cole-Cole (CC) function.[4,5,50] This function is usually applied to describe secondary relaxations in the glassy state of organic glass formers,[52] including *m-TOL*.[41]

III. RESULTS

Figure 1 displays the dielectric loss, ε'', of the *m-TOL* sample as a function of frequency, ν, for a series of the selected temperatures from the range 187–289 K. The spectral evolution of *m-TOL* from 187 K up to 210 K exhibits a bimodal form with an intense main peak feature and a weaker submerged peak at higher frequencies. Above $T_{\beta,disap}$ = 210 K, the dielectric spectrum of *m-TOL* changes its character from the bimodal form to a unimodal one due to the disappearance of the second peak feature. This spectral evolution is typical for type B glass formers of the operational Kudlik-Rössler classification of small molecular glass-formers.[53] In agreement with the previous studies on *m-TOL*, the main peak corresponds to the structural relaxation or the primary α process[39–42] and the newly observed weaker submerged peak at higher frequencies in the liquid state is ascribed to the faster secondary β relaxation.

A phenomenological analysis of the broadband dielectric spectra of *m-TOL* consists in the decomposition of the bimodal spectra by using the additive approach represented by Eq. (1). From fitting the dielectric spectra, the relaxation times $\tau_{HN,i}$, the shape parameters $\alpha_{HN,i}$, $\beta_{HN,i}$, and the corresponding relaxation strengths, $\Delta\varepsilon_i$, were determined for the individual relaxation modes in *m-TOL*—see Figs. 2–4. In the case of the main α relaxation, the low frequency flank of the measured loss peak does not have exactly slope 1; therefore, the general HN function with free α_{HN}, β_{HN} parameters is used. In addition, higher frequency data above about 1 GHz at relatively low temperatures above $T_{\beta,disap}$ are influenced by the measurement artifacts of the high-frequency (HF) device which limited the use of the HN function with free parameters to temperatures up to 255 K only (Fig. 3).

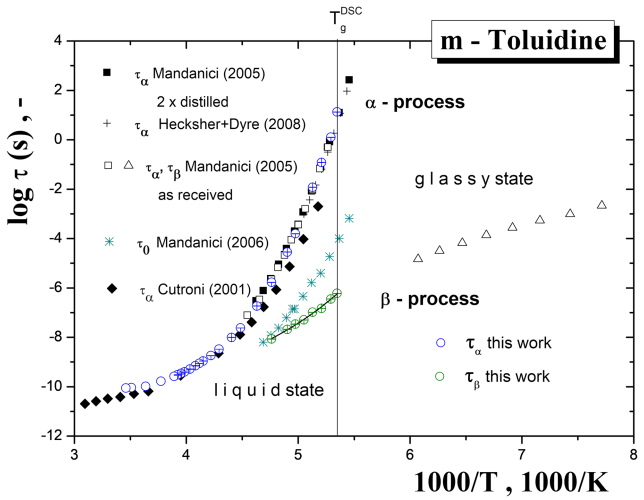

FIG. 2. Relaxation map of the measured relaxation time scales of the α and β processes τ_α, τ_β as a function of the inverse temperature (1000/T) for *m-TOL*. In addition, results from the literature are shown, namely, together with the α relaxation times for two-times distilled and for as received *m-TOL* measured in limited temperature ranges, i.e., 183–216 K and 193–220 K, respectively, from the studies of Mandanici *et al.*[41] and Hecksher *et al.*[43] as well as those from the work of Cutroni *et al.*[40] The observed β relaxation times τ_β above T_g together with the VFTH equation fit and the primitive $\tau_0 \equiv \tau_\beta$ times as estimated from the coupling model (CM) of liquids[42] are presented. The β relaxation times τ_β in the glassy state from 130 K up to 165 K[41,42] are also included. Error bars are included.

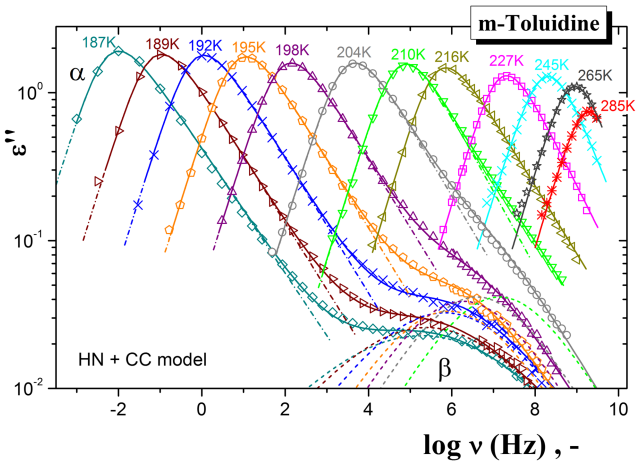

FIG. 1. Evolution of dielectric loss spectra of *m-TOL* over a wide frequency range 10^{-2}–$10^{9.5}$ Hz at selected temperatures (symbols: experimental data, solid lines: fits). The spectra in the temperature range 187–210 K were fitted by the sum of a HN and a CC function accounting for the primary α and secondary β relaxation, respectively. Above 210 K, the spectra could be fitted with the HN function.

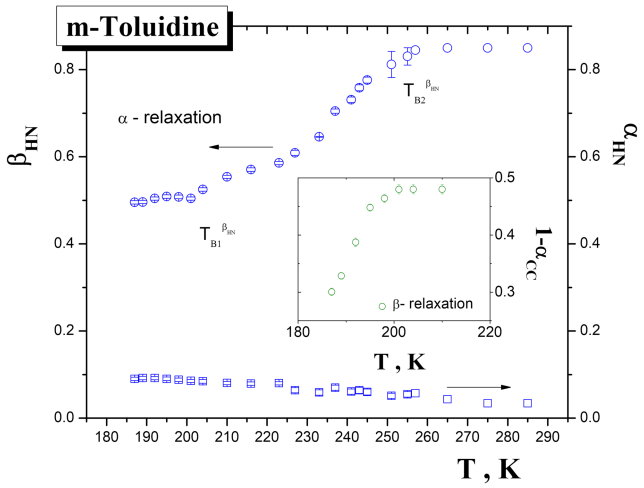

FIG. 3. The shape parameters β_{HN}, α_{HN}, and (1-α_{CC}) as a function of temperature in liquid *m-TOL* determined from the HN function fit for the primary α process or the CC function one for the secondary β process, respectively. Two characteristic BDS temperatures T_{Bi}^{HN} ($T_{B1}^{\beta HN} \cong 205$ K and $T_{B2}^{\beta HN} \cong 260$ K) are indicated at the cross section points of β_{HN}. Error bars are included.

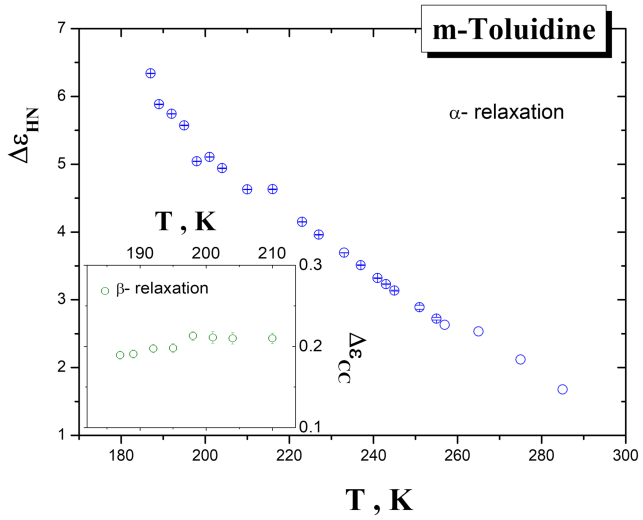

FIG. 4. Relaxation strengths for both relaxation processes in liquid *m-TOL*, $\Delta\varepsilon_{HN}$ and $\Delta\varepsilon_{CC}$, as a function of temperature as obtained from the HN function fit for the primary α process or the CC function one for the secondary β process, respectively. Error bars are included.

On the other hand, due to the high-frequency limitation of our experimental window, at the highest temperatures, a free-parameter fit using the HN function provides reliable results for β_{HN} up to 255 K only (Figs. 1 and 3). Above this temperature, β_{HN} had to be fixed to the value of 0.85 obtained from the free fit at 255 K. Note that choosing higher values of β_{HN}, such as 0.9 or 0.95, does not essentially alter the other spectral parameters, especially the relaxation time, $\tau_{HN,i}$, that varies by a few percent only. The additional symmetric peak was described by the CC function as usually applied for secondary processes[52] and as supported for the β relaxation in the glassy state of *m-TOL* in Ref. 41. Based on these facts, we used for the liquid *m-TOL* as the model function, the sum of the HN function and the CC one for the primary α relaxation or the secondary β process, respectively. At higher temperatures, at $T_{\beta,disap} > 210$ K, after the β relaxation peak becomes completely submerged under the dominating α peak, the spectra could be described consistently by a single HN function only.

Figure 2 displays the relaxation map of *m-TOL*, which consists of the measured relaxation times τ_α and τ_β in the *liquid* state as obtained from the additive fitting of the broadband dielectric spectra over a wide temperature interval from 187 to 289 K. In addition, the reported relaxation times for the primary α process[39–41,43] and the secondary β one in the glassy state[41,42] are given. They include the restricted LF-BDS study from 183 K up to 220 K by Mandanici *et al.*,[41,42] from 184 K up to 200 K by Hecksher *et al.*,[43] and another restricted LF-BDS + HF-BDS one from 193 to 323 K by Cutroni *et al.*[40] The mutual comparison of these individual time scales will be addressed in Sec. IV. In any case, the primary α process over the whole measured temperature range exhibits the non-Arrhenius character which can be described, e.g., by the Arrhenius regime at the highest temperatures and a super-Arrhenius zone in the lower temperature region in the supercooled liquid state down to the glass transition. Consequently, the originally proposed VFTH fits over limited temperature ranges[40,41] do not work over the whole temperature range. This aspect of the structural relaxation dynamics together with alternative descriptions in terms of various current dynamic models will be discussed in detail in Sec. IV.

The newly revealed secondary β relaxation in the liquid state of *m-TOL* shows a clear deviation from the Arrhenius behavior. Within the range 187 K–210 K, it can be described by the VFTH equation $\tau_\beta(T) = \tau_{\infty,\beta}[B_\beta{}^{VFTH}/(T - T_{0\beta}{}^{VFTH})]$ with the following parameters: $\tau_{\infty,\beta} = 8.3 \times 10^{-13}$s, $B_\beta{}^{VFTH} = 686$ K, and $T_{0\beta}{}^{VFTH} = 136$ K.

Figure 3 presents the temperature dependence of all three spectral shape parameters of both relaxations. Three distinct regions of the different behavior of the spectral shape parameter of the primary α process of the HN function, β_{HN}, are evident. Similar trends can be found for other organic glass-formers such as *benzophenone*[4] and *salol*.[23] The value of this parameter changes from about 0.52 in the first region up to about 0.85 in the last one. These individual regions of β_{HN} suggest two profound crossovers at the two characteristic BDS temperatures of the primary α process: $T_{B1}{}^{\beta HN} \cong 205$ K and $T_{B2}{}^{\beta HN} \cong 260$ K. As for the secondary β process, the values of the shape parameter ($1\text{-}\alpha_{CC}$) of the CC function over the limited range of 25 K above T_g have a continuously increasing trend with some saturation just above 200 K.

Next, Fig. 4 shows the temperature dependence of the relaxation strengths of both relaxation processes. The relaxation strength $\Delta\varepsilon_{HN}$ of the primary α relaxation process in *m-TOL* decreases rather continuously with increasing temperature. In the case of the secondary β relaxation, a slight increase of $\Delta\varepsilon_{CC}$ with temperature is found.

Finally, Fig. 5 presents the so-called Schönhals plot for the primary α process which provides information on the mutual model-free relation of two spectral parameters, namely, the spectral strength of structural relaxation, $\Delta\varepsilon_\alpha$, and the relaxation time, τ_α [Eq. (2)].[10] For *m-TOL*, three regions of distinct behavior are evident revealing two characteristic temperatures $T_{B1}{}^{SCH} \sim 220$ K and $T_{B2}{}^{SCH} \sim 265$ K. Interestingly, a

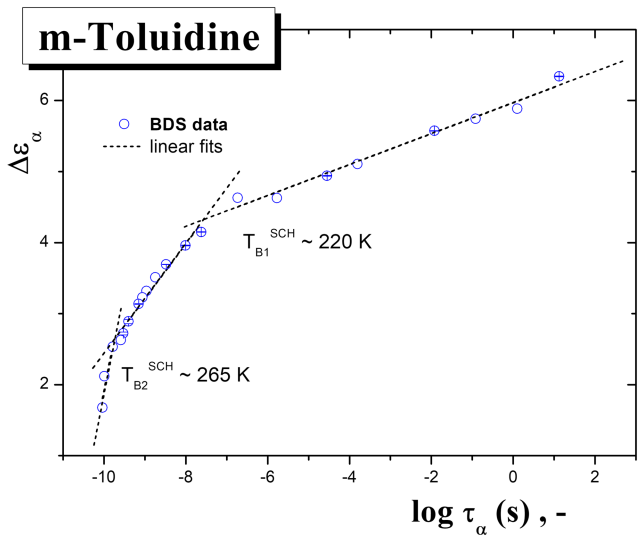

FIG. 5. Schönhals plot[10] for the primary α relaxation in *m-TOL*. The characteristic BDS temperatures $T_{B1}{}^{SCH}$ and $T_{B2}{}^{SCH}$ correspond to the two intersections points of linear fits.

comparison between the Schönhals plot and the shape parameter of the primary relaxation, β_{HN} (Fig. 3), suggests an approximate consistency of the three distinct regions in both dependencies.

IV. DISCUSSION

A. Phenomenological BDS results in comparison with the previous BDS data

The present LF-BDS and HF-BDS data on liquid *m-TOL* over a wide temperature range from 187 to 289 K can be confronted with the time scales and the shape parameters of both the relaxation processes as obtained from the previous more or less restricted BDS studies.[39–43]

Concerning the times scales, from Fig. 2, it follows that the relaxation times of the primary α process are in very good agreement with the reported data[41,43] over the common LF-BDS temperature range from T_g to ca. 215 K. These LF-BDS time scales are also in agreement with the relaxation times from a very recent light scattering study on *m-TOL* in the bulk state.[36] However, there are strong differences of the relaxation times in the restricted LF-BDS range from 193 to 220 K compared to the corresponding values from the earlier work (Ref. 40). On the other hand, above 220 K, both data sets are in a plausible agreement indicating a crossover at around 270 K from the super-Arrhenius regime into an approximate Arrhenius regime.

In addition, the reported[41,42] and present time scales for the secondary β process are also summarized in Fig. 4. The former consists of the secondary dynamics deeply in the glassy state from 130 K to 160 K = T_g − 27 K which exhibits the usual Arrhenius character.[46] Subsequently, as often made, a linear extrapolation into the supercooled liquid state over a rather extended temperature range towards the time scale of the primary α process provided the so-called merging or bifurcation temperature T_β = 216 K (Ref. 41). At the same time, the Stickel derivative analysis[9] of the *combined* dynamic data consisting of the LF-BDS structural relaxation time[41] and the relative high-temperature viscosity[32,33] gave the characteristic Stickel temperature ${T_B}^{ST} \sim 216$ K[41] or ${T_B}^{ST} = 212 \pm 3$ K[42] in apparent agreement with the T_β value suggesting the bifurcation of the secondary β process from the structural relaxation. However, this $T_\beta \cong {T_B}^{ST}$ finding is rather accidental because it is based on an implicit and unjustified assumption of the linearity of the secondary β time scale in the Arrhenius plot over the 56 K range from 160 K up to 216 K. This is confirmed by our detailed analysis of the broadband dielectric spectra which reveals the non-Arrhenius character of the secondary β relaxation in the liquid state of *m-TOL*. Such a non-Arrhenius character of the secondary relaxation above T_g was also found in several other supercooled liquids.[52,54–57]

Moreover, the authors[42] discussed the β process in both the glassy and supercooled liquid states in terms of the empirical relationship $E_\beta = 24 k_B T_g$[53] and the coupling model (CM) of structural relaxation[15] using the prediction $\tau_\beta = \tau_0$, where τ_0 is the so-called primitive relaxation time estimated from the primary α relaxation time and the spectral width parameter. The CM predicts the non-Arrhenius behavior of the secondary β time scale above T_g[57] as indeed observed in the present work (Fig. 2). However, only at the highest temperatures where the β process could be resolved, τ_β is found to agree with τ_0 and at lower temperatures deviations show up. Deviations of $\tau_\beta = \tau_0$ in Ref. 42 were taken as an indication that the detected secondary relaxation may not be a "genuine" Johari-Goldstein relaxation.[47]

Regarding the shape parameter of the primary α relaxation, the earlier LF-BDS + HF-BDS work over the temperature range 180–320 K by Cutroni *et al.*[40] presented a continuous increase of the stretching parameter, β_{KWW}, with a trend towards certain quasi-saturation in the high temperature region where the Arrhenius law for the time scale becomes valid. On the other hand, the recent LF-BDS study by Mandanici *et al.*[41] revealed a constant shape parameter of the structural relaxation suggesting the validity of the TTS principle over the restricted range of 187 K–215 K. Our finding of the three distinct regions in β_{HN} vs. T plot in Fig. 3 with the two characteristic BDS temperatures, ${T_{B1}}^{\beta HN}$ and ${T_{B2}}^{\beta HN}$, is quite different than the previous finding.[40] On the other hand, an approximate consistency of the first region in Fig. 3 exhibiting only a weak temperature increase of the β_{HN} parameter with the observation[41] of the validity of the TTS principle over a restricted temperature range, i.e., in the deeply supercooled liquid state from T_g = 187 K to 215 K ≅ ${T_{B1}}^{\beta HN}$ = 205 K seems to be evident.

B. The primary α process in terms of various dynamic models and their relationship with the thermodynamics

As suggested in the Introduction, several approaches attempt to describe the non-Arrhenius behavior of the structural relaxation in glass-forming organic systems. Figure 6 summarizes our application of the six current dynamic models on the structural relaxation time data of *m-TOL* shown in Fig. 2. The fit quality of all the used models is compared in terms of the corresponding differences between the experimental and fitted points in Fig. 7 and their standard deviations σ^2 are listed in the figure caption following Ref. 43. One group is formed by empirical expressions such as the VFTH[46] and power law (PL)[58] equations with divergence temperatures ${T_0}^{VFTH}$ and T_X, respectively. They can be combined with another VFTH law or with the Arrhenius expression[4–8] covering both the supercooled and normal liquid states. Another example is the more recent modified-VFTH (M-VFTH) expression.[20] A second class of phenomenological models includes various expressions based on certain physical pictures of glass-forming liquid dynamics with[13–19] or without[59–61] any characteristic dynamic temperature.

We start this section with a series of the simplest three-parameter models. Figures 6(a) and 7 demonstrate that the empirical VFTH equation[46] $\tau_\alpha(T) = \tau_{\infty,\alpha}[{B_\alpha}^{VFTH}/(T - {T_{0\alpha}}^{VFTH})]$ is not able to describe well the relaxation time over the whole measured temperature range. The fit quality is not satisfactory as revealed by the value $\sigma^2 = 0.046$. Deviations of $\tau_\alpha(T)$ from the VFTH behavior are often found in investigations of glass-forming liquids covering sufficiently broad frequency and temperature ranges.[8–10] A similar situation is valid for a combination of the VFTH equation with the Arrhenius one for the highest values of relaxation times. Here, the use of the VFTH law for the supercooled liquid region below

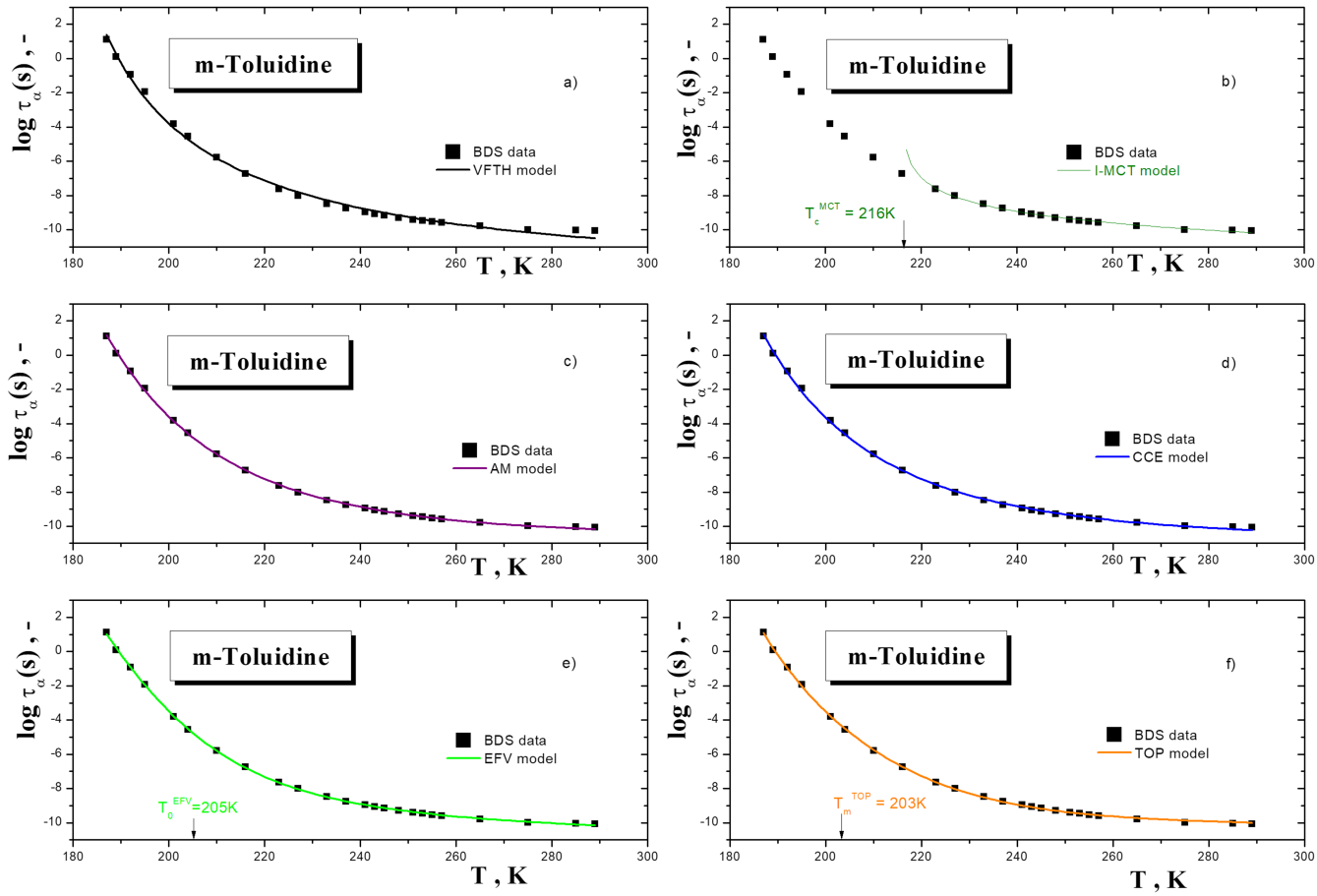

FIG. 6. Tests of (a) the standard VFTH equation[46] over the whole measured temperature range with the following fitting parameters: $\tau_{\infty,\alpha} = 5.4 \times 10^{-14}$ s, $B_\alpha{}^{\mathrm{VFTH}} = 801$ K, and $T_0{}^{\mathrm{VFTH}} = 163$ K; (b) the power law[58] or MCT model[17] over the moderately and high temperature range with the following fitting parameters: $\tau_{\infty,\alpha} = 4.1 \times 10^{-12}$ s, $\mu = 2.6$, and $T_X = T_c = 216$ K; (c) the activation energy distribution (AED) model over the whole measured temperature range with the following fitting parameters: $\tau_{\infty,\alpha} = 2.5 \times 10^{-11}$ s, $B^{\mathrm{AM}} = 257$ K, and $a = 7.7$; (d) the constraint configuration entropy (CCE) model over the whole measured temperature range with the following fitting parameters: $\tau_{\infty,\alpha} = 1.12 \times 10^{-11}$ s, $K = 2.46$, and $C = 1277$ K; (e) the extended free volume (EFV) model over the whole measured temperature range with the following fitting parameters: $\tau_{\infty,\alpha} = 5.4 \times 10^{-12}$ s, $B^{\mathrm{EFV}} = 195$, $T_0{}^{\mathrm{EFV}} = 205$ K, and $C = 4.4$; and finally, (f) the M-VFTH equation with the included fitting parameters: $\tau_{\infty,\alpha} = 4 \times 10^{-12}$ s, $E^* = 7.8$ kJ/mol, $B^{\mathrm{TOP}} = 1240$, $\kappa = 0.0497$, $T_m{}^{c} = 203$ K, $T_0{}^{\mathrm{TOP}} = 151$ K, and $T_A = 275$ K.

ca. 270 K and of the Arrhenius one above 270 K leads to an unphysically short pre-exponential factor for the former.

Another empirical equation is represented by the power law (PL)[58] being closely related to the prediction of the idealized mode coupling theory (I-MCT) of the liquid to glass transition,[17] which is argued to be valid for a large number of organic glass formers over rather higher temperature range,[62,63]

$$\tau_\alpha(T) = \tau_{\infty,\alpha}\left[\frac{(T - T_x)}{T_x}\right]^{-\mu}. \quad (3)$$

Here $\tau_{\infty,\alpha}$ is the pre-exponential factor, T_X is the characteristic dynamic PL or MCT temperature, and μ is the coefficient. As it is known, this model works well for the lower viscosity regime[17] so that we consider the data at $T > 220$ K (Fig. 5) for which rather satisfactory fit of the relaxation times of *m-TOL* [Fig. 6(b)] using Eq. (3) provides the characteristic dynamic crossover temperature of $T_X = T_c = 216$ K. The fit quality is essentially better as for the VTH model with the standard deviation of 0.003 60. Moreover, our value of $T_X = T_c$ is close to the estimate of 220 ± 5 K from the application of the I-MCT formalism to the dynamic data on *m-TOL* in the range 250–295 K from a time-resolved non-linear spectroscopy experiment, the optical Kerr effect (OKE).[35] Although in reality the relaxation time does not diverge at $T_X = T_c$, an analysis of the relaxation dynamics in terms of the extended mode coupling theory (E-MCT) removing this singularity shows the same crossover temperature in the supercooled liquid phase.[17] It is of interest that this dynamic crossover temperature, marking a dynamic transition from the liquid-like to solid-like dynamic behavior of the supercooled liquid, is quite close to the characteristic BDS temperature $T_{B1}{}^{\beta HN} = 205$ K from the present BDS study.

Finally, a subgroup of two further three-parameter equations is represented by the activation energy distribution hopping model by Avrami and Milchev (AM),[61]

$$\tau_\alpha(T) = \tau_{\infty,\alpha}\left[\exp\left(B^{AM}/T\right)^a\right], \quad (4)$$

where $\tau_{\infty,\alpha}$ is the pre-exponential factor, and B^{AM} and a are constants, and by the double exponential[59] or constraint configuration entropy (CCE) model by Mauro *et al.*,[60]

$$\tau_\alpha(T) = \tau_{\infty,\alpha}\exp\left[\frac{K}{T}\exp(C/T)\right], \quad (5)$$

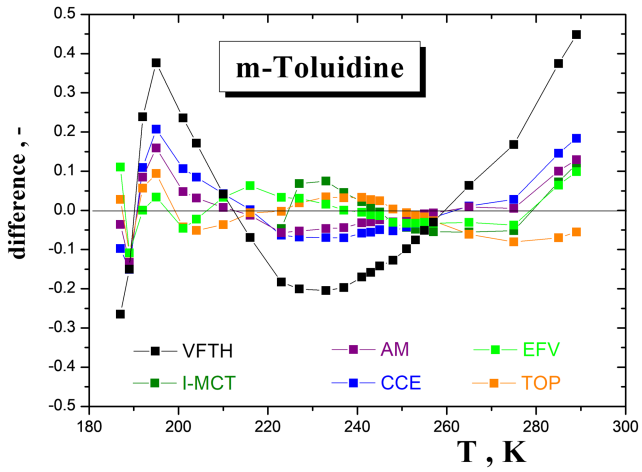

FIG. 7. Comparison of the corresponding differences between the logarithms of the experimental and the fitting relaxation times from the used six models. The values of the standard deviations σ^2 calculated from these differences are as follows: VFTH model 0.046; I-MCT model: 0.00360; AM model: 0.00436; CCE model: 0.00897; EFV model: 0.00259; and M-VFTH equation of the TOP model: 0.00249.

where $\tau_{\infty,\alpha}$ is the pre-exponential factor, and K and C are constants. The corresponding fits are shown in Figs. 6(c) and 6(d) with the standard deviations in Fig. 7: 0.004 36 vs. 0.008 97. These equations quite satisfactorily describe the BDS data of *m-TOL* over the entire measured liquid state with the smaller standard deviation for the AM model. However, the authors of the CCE model argue that the AM formula has the unphysical high temperature limit.[60] Thus, although the CCE model works better for some organic glass formers in comparison with the "basic" VFTH model,[64] it does not provide any characteristic temperature for comparison with and interpretation of the two observed characteristic BDS anomalies found in the present work for the structural relaxation in *m-TOL*.

Next, Fig. 6(e) displays a test of a four-parameter description of the liquid dynamics, namely, the extended free volume (EFV) model of Cohen and Grest,[13]

$$\tau_\alpha(T) = \tau_{\infty,\alpha} \exp\left\{B^{EFV} / \left\{\left(T - T_0^{EFV}\right) + \left[\left(T - T_0^{EFV}\right)^2 + CT\right]^{1/2}\right\}\right\}. \quad (6)$$

Here $\tau_{\infty,\alpha}$ is the pre-exponential factor, $T_0{}^{\mathrm{EFV}}$ is the characteristic EFV temperature, and B^{EFV} and C are material constants. Obviously, this expression describes the temperature dependence of the structural relaxation very well with the standard deviation of 0.002 59 with $T_0{}^{\mathrm{EFV}} = 205 \pm 2$ K. Since this value of the characteristic EFV temperature agrees with the first characteristic BDS one $T_{\mathrm{B1}}{}^{\beta\mathrm{HN}}$, it suggests that the onset of a strong change in the shape parameter β_{HN} of the structural relaxation may be interpreted in terms of the EFV model as being related to of the free volume percolation in *m-TOL* at ca. $1.1T_{\mathrm{g}}$.

Finally, we focus on a test of the two-order parameter (TOP) model because of its potential to give some simultaneous insight into several spectral parameters of the BDS as well as positron annihilation lifetime spectroscopy (PALS) findings.[21–26] The TOP model is based on the *solid* - and *liquid*-like domain pictures of the glass-forming liquids and the structural relaxation times over the very wide T range including both the *supercooled* and *normal* liquid states can be described in terms of the modified VFTH (M-VFTH) equation[20]

$$\tau_\alpha(T) = \tau_{\infty,\alpha} \exp\left[E^*/RT\right] \exp\left[B^{TOP} f(T) / \left(T - T_0^{TOP}\right)\right]. \quad (7)$$

Here $\tau_\alpha(T)$ is the relaxation time, $\tau_{\infty,\alpha}$ is the pre-exponential factor, E^* is the activation energy above $T_{\mathrm{A}} \geq T_{\mathrm{m}}$, $T_0{}^{\mathrm{TOP}}$ is the divergence temperature, B^{TOP} is the coefficient, and a probability function $f(T)$ for the *solid*-like domains is given as

$$f(T) = \frac{1}{\exp\left[\kappa\left(T - T_m^c\right)\right] + 1}, \quad (7a)$$

where κ reflects the sharpness of $f(T)$ and $T_{\mathrm{m}}{}^{\mathrm{c}}$ is the characteristic TOP temperature at which the free energy of crystallizing or non-crystallizing liquids is equal to the solid state energy $\Delta G_{\mathrm{lq}} = \Delta G_{\mathrm{sol}}$. The TOP model provides the physical picture of any glass-forming compound from the *glassy* state over *supercooled* liquid to *normal* liquid state in terms of the temperature dependence of the *solid*-like domain probability function $f(T)$.

Figure 6(f) demonstrates a description of the primary α relaxation times of *m-TOL* using the M-VFTH equation with the smallest standard deviation of 0.002 49, somewhat better than the EFV model. The three characteristic TOP temperatures as obtained from a fit with Eq. (2) are $T_0{}^{\mathrm{TOP}} = 151 \pm 1.5$ K, $T_{\mathrm{m}}{}^{\mathrm{C}} = 203 \pm 1.7$ K, and $T_{\mathrm{A}} = 275$ K which can be compared with the characteristic thermodynamic and dynamic temperatures. Concerning the former type of comparison, the divergence temperature $T_0{}^{\mathrm{TOP}} = 151$ K is significantly higher than the divergence VFTH temperature from fitting the deeply supercooled liquid region LF-BDS data: $T_{0\alpha}{}^{\mathrm{VFTH}} = 138$ K, together with a very small pre-exponent.[41,42] On the other hand, $T_0{}^{\mathrm{TOP}}$ is in a plausible agreement with the characteristic thermodynamic Kauzmann temperature $T_{\mathrm{K}} = 151$ K[28] and 157 K.[65] This mutual $T_0{}^{\mathrm{TOP}} \cong T_{\mathrm{K}}$ relationship indicates the common origin of the dynamic and thermodynamic phenomena and seems to support the approaches assuming a true divergence temperature below T_{g} for *m-TOL*. This finding seems to be consistent with the very recent critical evaluation of various divergent vs. non-divergent dynamic approaches in favor of the former ones.[66]

Concerning the latter type of comparison, the remaining characteristic TOP temperatures agree quite well with those for the temperature evolution of the shape parameter β_{HN} of the primary α relaxation process and the following relations can be found: $T_{\mathrm{B1}}{}^{\beta\mathrm{HN}} \cong T_{\mathrm{m}}{}^{\mathrm{c}}$ and $T_{\mathrm{B2}}{}^{\beta\mathrm{HN}} \approx T_{\mathrm{A}}$. Recently, analogous relations were found also in our detailed BDS study on *salol*[23] and benzophenone.[4,67] Figure 8 demonstrates that a slight change of the shape parameter β_{HN} in the first region from T_{g} up to $T_{\mathrm{B1}}{}^{\beta\mathrm{HN}} = 205$ K can be related to the dominating *solid*-like domains in the deeply supercooled liquid *m-TOL*. Next, on crossing the characteristic BDS temperature $T_{\mathrm{B1}}{}^{\beta\mathrm{HN}}$, which lies in the vicinity of the characteristic TOP temperature $T_{\mathrm{m}}{}^{\mathrm{c}}$, the found significant variance of the shape of the primary α process via a narrowing of the time scale distribution can be ascribed to the onset of the dominance of the *liquid*-like domains in the weakly supercooled liquid *m-TOL*. On further increase of the temperature, the approximate constancy of the

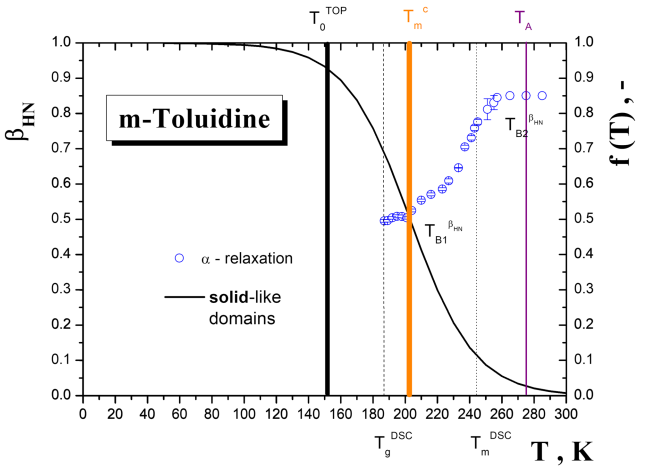

FIG. 8. Interpretation of the changes in the shape parameter β_{HN} of the structural relaxation at $T_{B1}{}^{\beta HN}$ and $T_{B2}{}^{\beta HN}$ in terms of the characteristic TOP temperatures $T_o{}^{TOP}$, $T_m{}^c$, and T_A of the TOP model. Both the basic thermodynamic temperatures $T_g{}^{DSC}$ and $T_m{}^{DSC}$ from Ref. 28 are also included.

shape parameter $\beta_{HN} = 0.85$ above $T_{B2}{}^{\beta HN} \cong 260$ K is not too distant from the Arrhenius temperature $T_A \cong 275$ K and might be related to the almost disappearance of the *solid*-like domains.

In summary of this section, by a quantitative comparison of the six current dynamic models on the basis of the standard-deviation analysis of the structural relaxation times, as could be expected we find that in general the models with more parameters are better able to describe the whole temperature range of the structural relaxation time in *m-TOL*. In addition to this basic reflection of the experimental relaxation data, the corresponding characteristic dynamic temperatures, i.e., $T_c{}^{MCT}$, $T_0{}^{EFV}$, and $T_m{}^c$ from the afore-mentioned analyses of the structural relaxation time in *m-TOL* seem to provide reasonable physical interpretations of the changes in further relaxation parameter, i.e., spectral shape one of the primary α process, β_{HN}. Thus, the dramatic change at $T_{B1}{}^{\beta HN}$ is connected with the underlying controlling aspect such as a solid-like to liquid-like dynamic phase transition in the density fluctuation within the MCT model, an onset of the percolating free volume in the EFV model, and an onset of the dominancy of *liquid*-like domains within the TOP model. In other words, it seems that these signatures are not only plausible but also mutually consistent.

V. CONCLUSIONS

We have presented the dynamic properties of *m-TOL* from a broadband dielectric spectroscopic (BDS) study over a wide temperature and frequency range in the *liquid* state. The detailed phenomenological analysis of the broadband dielectric spectra in terms of the additive HN and CC function models revealed for the first time the secondary β process in the strongly supercooled *liquid* state disappearing ca. 25 K above T_g with the non-Arrhenius behavior of its relaxation time, which can be accounted for by the VFTH equation. The primary α-relaxation extended by including the new HF data exhibits the non-Arrhenius character of the relaxation time, which can be successfully described by a set of current three-, four-, and six-parameter models with the corresponding characteristic temperatures such as three-parameter MCT, the four-parameter EFV model, and the six-parameter TOP model with a preference for equations with more parameters. Moreover, three regions of a strongly distinct behavior of the spectral shape parameter β_{HN} marked by the characteristic BDS temperatures $T_{B1}{}^{\beta HN} \cong 205$ K and $T_{B2}{}^{\beta HN} \cong 260$ K were found. The first change of the shape parameter can be related to a number of the characteristic dynamic temperatures of these models such as $T_c{}^{MCT}$, $T_0{}^{EFV}$, and $T_m{}^c$, while the other one lies in the vicinity of the Arrhenius temperature T_A of the TOP model. Overall, we find mutual relationships between characteristic temperatures of the spectral shape of the primary relaxation and of model descriptions of its time scale in *m-TOL*. Our results indicate that a plausible and consistent physical interpretation of the pronounced change of β_{HN} at $T_{B1}{}^{\beta HN}$ is possible in terms of the solid-like to liquid-like dynamic phase transition in the density fluctuation within the MCT model, an onset of the percolating free volume in the EFV model, and an onset of the dominancy of *liquid*-like domains within the TOP model.

ACKNOWLEDGMENTS

The first and last authors thank Experimental Physics V at the University of Augsburg, Germany for allowance and experimental and financial support to perform this dielectric study and the VEGA agency, Slovakia for support by the Grant Nos. 2/0030/16 (J.B.) and APVV-16-0369 (J.B.).

[1] M. D. Ediger, C. A. Angell, and S. R. Nagel, J. Phys. Chem. B **100**, 13200 (1996).
[2] C. A. Angell, K. L. Ngai, G. B. McKenna, P. F. McMillan, and S. W. Martin, J. Appl. Phys. **88**, 3113 (2000).
[3] P. G. DeBenedetti and F. H. Stillinger, Nature **410**, 259 (2001).
[4] P. Lunkenheimer, U. Schneider, R. Brand, and A. Loidl, Contemp. Phys. **41**, 15 (2000); P. Lunkenheimer, M. Köhler, S. Kastner, and A. Loidl in *Structural Glasses and Supercooled Liquids*, edited by P. G. Wolynes and V. Lubchenko (Wiley, Hoboken, 2012), Chap. 3, p. 115.
[5] *Broadband Dielectric Spectroscopy*, edited by F. Kremer and A. Schönhals (Springer, Berlin, 2002).
[6] A. J. Barlow, J. Lamb, and A. J. Matheson, Proc. R. Soc. London, Ser. A **292**, 322 (1966); D. J. Plazek and J. H. Magill, J. Chem. Phys. **45**, 3038 (1966).
[7] K. L. Ngai, J. H. Magill, and D. J. Plazek, J. Chem. Phys. **112**, 1887 (2000).
[8] A. Schönhals, F. Kremer, A. Hofmann, E. W. Fischer, and E. Schlosser, Phys. Rev. Lett. **70**, 3459 (1993).
[9] F. Stickel, E. W. Fischer, and R. Richter, J. Chem. Phys. **102**, 6251 (1995); F. Stickel, E. W. Fischer, R. Richert, and E. W. Fischer, *ibid.* **104**, 2043 (1996); C. Hansen, F. Stickel, R. Richter, and E. W. Fischer, *ibid.* **108**, 6408 (1998).
[10] A. Schönhals, Europhys. Lett. **56**, 815 (2001).
[11] C. Leon and K. L. Ngai, J. Phys. Chem. B **103**, 4045 (1999); K. L. Ngai and C. M. Roland, Polymer **43**, 567 (2002).
[12] A. Alegría, J. Colmenero, P. O. Mari, and I. A. Campbell, Phys. Rev. E **59**, 6888 (1999).
[13] M. H. Cohen and G. S. Grest, Phys. Rev. B **20**, 1077 (1979); G. S. Grest and M. H. Cohen, *ibid.* **28**, 4113 (1980); M. H. Cohen and G. S. Grest, Adv. Chem. Phys. **48**, 455 (1981).
[14] M. Paluch, R. Casalini, and C. M. Roland, Phys. Rev. E **67**, 021508 (2003).
[15] K. L. Ngai, Comments Solid State Phys. **9**, 141 (1979); J. Phys.: Condens. Matter **15**, S1107 (2003).
[16] R. Casalini, K. L. Ngai, and C. M. Roland, Phys. Rev. B **68**, 014201 (2003).
[17] W. Götze and L. Sjögren, Rep. Prog. Phys. **55**, 241 (1992); W. Götze, J. Phys.: Condens. Matter **11**, A1 (1999).

[18]E. Eckstein, J. Qian, R. Hentschke, T. Thurn-Albert, W. Steffen, and E. W. Fischer, J. Chem. Phys. **113**, 4751 (2000).
[19]E. Fischer and A. Sakai, AIP Conf. Proc. **469**, 325 (1999); E. W. Fischer, A. Bakai, A. Patkowski, W. Steffen, and L. Reinhardt, J. Non-Cryst. Solids **307-310**, 584 (2002).
[20]H. Tanaka, J. Phys.: Condens. Matter **10**, L207 (1998); **11**, L159 (1999); J. Chem. Phys. **111**, 3175–3182 (1999); J. Non-Cryst. Solids **351**, 3371, 3385, and 3396 (2005).
[21]J. Bartoš, V. Majerník, M. Iskrová, O. Šauša, J. Krištiak, P. Lunkenheimer, and A. Loidl, J. Non-Cryst. Solids **356**, 794 (2010).
[22]J. Bartoš, O. Šauša, M. Köhler, H. Švajdlenková, P. Lunkenheimer, J. Krištiak, and A. Loidl, J. Non-Cryst. Solids **357**, 376 (2011).
[23]J. Bartoš, M. Iskrová, M. Köhler, R. Wehn, O. Šauša, P. Lunkenheimer, J. Krištiak, and A. Loidl, Eur. Phys. J. E **34**, 104 (2011).
[24]J. Bartoš, G. A. Schwartz, O. Šauša, A. Alegría, J. Krištiak, and J. Colmenero, J. Non-Cryst. Solids **356**, 782 (2010).
[25]J. Bartoš, O. Šauša, G. A. Schwartz, A. Alegría, J. M. Alberdi, A. Arbe, J. Krištiak, and J. Colmenero, J. Chem. Phys. **134**, 164507 (2011).
[26]J. Bartoš, M. Iskrová-Miklošovičová, D. Cangialosi, A. Alegría, O. Šauša, H. Švajdlenková, A. Arbe, J. Krištiak, and J. Colmenero, J. Phys.: Condens. Matter **24**, 155104 (2012).
[27]V. Legrand, M. Descamps, and C. Alba-Simionesco, Thermochim. Acta **307**, 77 (1997).
[28]C. Alba Simionesco, J. Fan, and C. A. Angell, J. Chem. Phys. **110**, 5262 (1999).
[29]D. Morineau, C. Alba-Simionesco, M. C. Bellissent-Funel, and M. F. Lauthié, Europhys. Lett. **43**, 195 (1998).
[30]D. Morineau and C. Alba-Simionesco, J. Chem. Phys. **109**, 8494 (1998).
[31]R. Chelli, G. Cardini, P. Procacci, R. Righini, and S. Califano, J. Chem. Phys. **119**, 357 (2003).
[32]C. Dreyfus, A. Aoudi, R. M. Pick, T. Berger, A. Patkowski, and W. Steffen, Europhys. Lett. **42**, 55 (1998).
[33]L. Carpentier, R. Decressain, and M. Descamp, J. Chem. Phys. **121**, 6470 (2004).
[34]A. Aoudi, C. Dreyfus, M. Massot, R. M. Pick, T. Berger, W. Steffen, A. Patkowski, and C. Alba-Simionesco, J. Chem. Phys. **112**, 9860 (2000).
[35]R. Torre, P. Bartolini, M. Ricci, and R. M. Pick, Europhys. Lett. **52**, 324 (2000).
[36]T. Blochowicz, E. Gouirand, S. Schramm, and B. Stühn, J. Chem. Phys. **138**, 114501 (2013).
[37]L. Gomez, S. Correzzi, G. Monaco, R. Verbeni, and D. Fioretto, Phys. Rev. Lett. **94**, 155702 (2005).
[38]A. Faraone, K. Hong, L. R. Kneller, M. Ohl, and J. R. D. Cople, J. Chem. Phys. **136**, 104502 (2012).
[39]M. Cutroni, M. Mandanici, R. Pelster, and A. Spanoudaki, AIP Conf. Proc. **513**, 98 (2000).
[40]M. Cutroni, A. Mandanici, A. Spanoudaki, and R. Pelster, J. Chem. Phys. **114**, 7118 (2001).
[41]A. Mandanici, M. Cutroni, and R. Richert, J. Chem. Phys. **122**, 084508 (2005).
[42]A. Mandanici, R. Richert, M. Cutroni, X. Shi, S. A. Hutcheson, and G. B. McKenna, J. Non-Cryst. Solids **352**, 4729 (2006).
[43]T. Hecksher, A. I. Nielsen, N. B. Olsen, and J. C. Dyre, Nat. Phys. **4**, 737 (2008).
[44]M. Cutroni and A. Mandanici, J. Chem. Phys. **114**, 7124 (2001).
[45]A. Mandanici, X. Shi, G. B. McKenna, and M. Cutroni, J. Chem. Phys. **122**, 114501 (2005).
[46]H. Vogel, Phys. Z. **22**, 645 (1921); G. S. Fulcher, J. Am. Ceram. Soc. **8**, 339 (1925); G. Tamman and W. Hesse, Z. Anorg. Allg. Chem. **156**, 245 (1926).
[47]G. P. Johari and M. Goldstein, J. Chem. Phys. **53**, 2372 (1970).
[48]R. Böhmer, M. Maglione, P. Lunkenheimer, and A. Loidl, J. Appl. Phys. **65**, 901 (1989).
[49]U. Schneider, P. Lunkenheimer, A. Pimenov, R. Brand, and A. Loidl, Ferroelectrics **249**, 89 (2001).
[50]S. Havriliak and S. S. Negami, Polymer **8**, 161 (1967).
[51]A. Boersma, J. van Turnhout, and M. Wübbenhorst, Macromolecules **31**, 7453 (1998); K. Schröter, R. Unger, S. Reissig, F. Garwe, S. Kahle, M. Beiner, and E. Donth in *Dielectric and Mechanical Relaxation on Materials* (Hanser, Münich, 1997), p. 57; R. Diaz-Calleja, Macromolecules **33**, 8924 (2000).
[52]S. Kastner, M. Köhler, Y. Goncharov, P. Lunkenheimera, and A. Loidl, J. Non-Cryst. Solids **357**, 510 (2011).
[53]A. Kudlik, S. Benkhof, T. Blochowicz, T. Tschirwitz, and E. Rössler, J. Mol. Struct. **479**, 201 (1999).
[54]K. L. Ngai, P. Lunkenheimer, C. Leon, U. Schneider, R. Brand, and A. Loidl, J. Chem. Phys. **115**, 1405 (2001).
[55]M. Paluch, C. M. Roland, S. Pawlus, J. Ziolo, and K. L. Ngai, Phys. Rev. Lett. **91**, 115701 (2003).
[56]T. Blochowicz and E. A. Roessler, Phys. Rev. Lett. **92**, 225701 (2004).
[57]K. L. Ngai and M. Paluch, J. Chem. Phys. **120**, 857 (2004).
[58]P. Taborek, R. N. Kleinman, and D. J. Bishop, Phys. Rev. B **34**, 1835 (1986).
[59]S. C. Waterton, J. Soc. Glass Technol. **16**, 244 (1932).
[60]J. C. Mauro, Y. Yue, A. J. Ellison, P. K. Gupta, and D. C. Allan, Proc. Natl. Acad. Sci. U. S. A. **106**, 19780 (2009).
[61]I. Avramov and A. Milchev, J. Non-Cryst. Solids **104**, 253 (1988); I. Avramov, *ibid.* **351**, 3163 (2005).
[62]F. Mallamace, C. Branca, C. Corsaro, N. Leone, J. Spooren, S. H. Chen, and H. E. Stanley, Proc. Natl. Acad. Sci. U. S. A. **107**, 22457 (2010).
[63]F. Mallamace, C. Corsaro, H. E. Stanley, and S. H. Chen, Eur. Phys. J. E **34**, 94 (2011).
[64]P. Lunkenheimer, S. Kastner, M. Köhler, and A. Loidl, Phys. Rev. E **81**, 051504 (2010).
[65]C. A. Angell, J. Res. Natl. Inst. Stand. Technol. **102**, 171 (1997).
[66]J. C. Martinez-Garcia, S. J. Rzoska, A. Drzozd-Rzoska, J. Martinez-Garcia, and J. C. Mauro, Sci. Rep. **4**, 5160 (2014).
[67]P. Lunkenheimer, L. C. Pardo, M. Köhler, and A. Loidl, Phys. Rev. E **77**, 031506 (2008). P. Lunkenheimer, H. Švajdlenková, J. Bartoš *et al.* (unpublished).